

Diffuse Galactic Soft Gamma-Ray Emission

S. E. Boggs^{1,2}, R. P. Lin², and S. Slassi-Sennou

Space Sciences Laboratory, University of California, Berkeley, CA 94720

and

W. Coburn and R. M. Pelling

Center for Astrophysics and Space Sciences, University of California, La Jolla, CA 92093

Received _____; accepted _____

¹Millikan Postdoctoral Research Fellow;

present address: Space Radiation Laboratory, California Institute of Technology, MC 220-47, Pasadena, CA 91125; boggs@srl.caltech.edu

²Department of Physics, University of California, Berkeley, CA 94720

ABSTRACT

The Galactic diffuse soft gamma-ray (30-800 keV) emission has been measured from the Galactic Center by the HIREGS balloon-borne germanium spectrometer to determine the spectral characteristics and origin of the emission. The resulting Galactic diffuse continuum is found to agree well with a single power-law (plus positronium) over the entire energy range, consistent with RXTE and COMPTEL/CGRO observations at lower and higher energies, respectively. We find no evidence of spectral steepening below 200 keV, as has been reported in previous observations. The spatial distribution along the Galactic ridge is found to be nearly flat, with upper limits set on the longitudinal gradient, and with no evidence of an edge in the observed region. The soft gamma-ray diffuse spectrum is well modeled by inverse Compton scattering of interstellar radiation off of cosmic-ray electrons, minimizing the need to invoke inefficient nonthermal bremsstrahlung emission. The resulting power requirement is well within that provided by Galactic supernovae. We speculate that the measured spectrum provides the first direct constraints on the cosmic-ray electron spectrum below 300 MeV.

Subject headings: gamma-rays: observations — ISM: cosmic rays — Galaxy: center

1. Introduction

Galactic diffuse gamma-ray emission provides information on the origin, propagation, and interaction of cosmic-ray electrons within the Galaxy, complementary to the knowledge gained from direct observation of the cosmic-ray electrons in the Solar vicinity, and nonthermal radio emission from interactions with Galactic magnetic fields. The cosmic-ray electron spectrum has been directly measured above a few GeV (Golden et al. 1984, Golden et al. 1994, Taira et al. 1993), and extended down to 300 MeV by radio synchrotron observations (Weber 1983). Below 300 MeV, the electron spectrum must be constrained by the gamma-ray observations themselves. Observations and mapping of this diffuse continuum also provides a background which, as soft gamma-ray observations become more sensitive, will be important for the detailed study of faint sources.

A number of satellite and balloon instruments have measured the Galactic diffuse continuum in the hard X-ray/soft gamma-ray bands, e.g., OSO 7 [7-40 keV] (Wheaton 1976), HEAO 1 [2-50 keV] (Worrall et al. 1982), SMM [0.3-8.5 MeV] (Harris et al. 1990), GRIS [20 keV - 10 MeV] (Gehrels & Tueller 1993), COMPTEL/CGRO [1-30 MeV] (Strong et al. 1996), Ginga [2-16 keV] (Yamasaki et al. 1996), OSSE/CGRO [70 keV - 4 MeV] (Purcell et al. 1995), RXTE [3-35 keV] (Valinia & Marshall 1998). These observations have revealed nonthermal emission distributed along a Galactic ridge that extends $\pm 60^\circ$ in longitude.

The hard X-ray/soft gamma-ray continuum is believed to be dominated by three components (Strong et al. 1995, Skibo & Ramaty 1993): nonthermal bremsstrahlung from cosmic-ray interactions with the interstellar gas, inverse Compton scattering of the interstellar radiation (optical, infrared, and cosmic microwave background) off of the cosmic-ray electrons, and positronium continuum from the annihilation of Galactic positrons below 511 keV. At lower energies ($< 10\text{keV}$) thermal emission from the hot ISM

dominates, while at higher energies ($> 100\text{MeV}$) π^0 decay emission dominates.

Models of the nonthermal bremsstrahlung and inverse Compton components (Strong et al. 1995, Skibo & Ramaty 1993) predict that bremsstrahlung dominates in the MeV range, though inverse Compton still provides a significant fraction of the total flux; at lower energies, however, bremsstrahlung is highly inefficient compared to ionization and Coulomb collision losses (e.g., Strong et al. 1995, Skibo, Ramaty & Purcell 1996), and the bremsstrahlung spectrum drops rapidly; therefore, inverse Compton is expected to dominate below 1 MeV. The combination of the bremsstrahlung and inverse Compton, however, should produce a very smooth continuum from 10 keV to 30 MeV (Strong et al. 1995, Skibo & Ramaty 1993), though the addition of the positronium continuum will produce a well-defined spectral jump at 511 keV. This smooth continuum makes it difficult to distinguish the relative contributions of the bremsstrahlung and inverse Compton emission from the spectrum alone.

The spatial distributions of the two components, however, should be significantly different. Due to the diffuse cosmic background, and the large scale heights of the interstellar optical and IR emission and the cosmic-ray electrons compared to the interstellar gas, the scale height of the inverse Compton component should be significantly larger than the scale height of the bremsstrahlung emission. The presence of both broad and narrow scale height components has been confirmed in the 1-30 MeV energy band by COMPTEL/CGRO (Strong et al. 1996) and in the 3-35 keV band by RXTE (Valinia & Marshall 1998), adding strong support to the two-component model. These observations also suggest a smooth continuum from 10 keV to 30 MeV, with measured photon indices of 1.8 (RXTE) and ~ 2.0 (COMPTEL/CGRO). This smooth continuum is consistent with models of the combined bremsstrahlung and inverse Compton emission (e.g., Strong et al. 1995, Skibo & Ramaty 1993).

Observations in the 50 keV - 4 MeV energy band with OSSE/CGRO, the energy range between COMPTEL/CGRO and RXTE, have brought into question this simple two component (plus positronium) model of the Galactic diffuse continuum (Purcell et al. 1995). These observations suggest a strong steepening of the diffuse spectrum below 200 keV which is difficult to explain in terms of this model. The inverse Compton emission at these energies is produced predominantly by higher energy ($> GeV$) electrons, the spectrum of which has been well constrained by Galactic synchrotron radio emission (Weber 1983), so that an inverse Compton origin for a hard X-ray excess is highly unlikely (Skibo 1997). Furthermore, due to the inefficiency of bremsstrahlung emission below 1 MeV, the energetics required to produce such hard X-ray emission exceeds the total power expected from Galactic supernovae (Skibo 1997).

Measurements of the diffuse Galactic hard X-ray and soft gamma-ray emission are inherently upper limits due to the large number of hard X-ray compact sources in the Galactic Center region and the inevitable source confusion. Difficulty arises because non-imaging instruments with large fields-of-view (FOVs) are most sensitive to the diffuse continuum but are highly susceptible to compact source confusion, whereas imaging instruments or instruments with narrow FOVs are able to measure the compact sources individually, but are not as sensitive to the diffuse emission. Scans by wide and moderate FOV instruments (e.g., HEAO 1, SMM), and coordinated observations between imaging instruments and wider FOV instruments (e.g., OSSE/CGRO & SIGMA) have been performed to subtract out the compact source contributions, but still show hard X-ray spectra that are easiest to explain by compact source confusion.

The HIREGS spectrometer observed the Galactic Center region in January 1995 during a long duration balloon flight from Antarctica (Boggs et al. 1998). HIREGS is a wide FOV instrument (21° FWHM), but three sets of narrow FOV passive hard X-ray collimators

($3.7^\circ \times 21^\circ$ FWHM) were added over half of the twelve detectors for this flight. HIREGS thus simultaneously performed wide and narrow FOV observations of the same region, allowing the direct measurement and separation of compact source spectra and the Galactic diffuse.

In this paper we present the analysis and results of the HIREGS measurements of the diffuse Galactic emission in the 30-800 keV band from the Galactic Center region. Our observations are consistent with a single power-law (plus positronium) over the entire energy band, with a spectral index that agrees well with RXTE observations at lower energies, and COMPTEL/CGRO observations at higher energies. These results are inconsistent with previous observations of spectral steepening below 200 keV (e.g., OSSE/CGRO), which are most likely due to compact source contamination. Upper limits on the longitudinal gradients along the Galactic ridge are presented. We discuss implications of the soft gamma-ray diffuse Galactic emission on the cosmic-ray electron spectrum.

2. Instrument and Observations

HIREGS is a high-resolution spectrometer (2.0 keV FWHM at 592 keV) covering three orders of magnitude in energy, from 20 keV to 17 MeV. The instrument is an array of twelve high-purity 6.7-cm diameter by 6.1-cm height coaxial germanium detectors designed for long duration balloon flights. The array is enclosed on the sides and bottom by a 5-cm thick BGO shield, and collimated to a 21° FWHM FOV by a 10-cm thick CsI collimator. The instrument (Pelling et al. 1992), and the flight (Boggs et al. 1998) are described in greater detail elsewhere.

Passive molybdenum (0.15 mm) collimators were designed for this flight to limit the hard X-ray ($< 200\text{keV}$) FOV for half of the detectors to $3.7^\circ \times 21^\circ$ FWHM (Figure 1).

Three sets of these collimators were inserted in the main collimator and slanted in parallel directions, providing three parallel but separate FOVs. Therefore, the instrument had four different hard X-ray FOVs for any given pointing: one wide 21° FOV, and three narrow $3.7^\circ \times 21^\circ$ FOVs.

Spectra were collected for 30 minute periods, alternating between source observations and background observations at the same horizon elevation. The backgrounds were taken at least one FOV width off of the Galactic Plane to avoid source contamination, and were alternated to the east and west of the source pointings to avoid any systematic errors. Despite these precautions, there is a soft source ($< 40\text{keV}$) contaminating the westerly background pointings. This source affected the preliminary analysis of this data (Boggs et al. 1997), allowing misidentification of the compact sources and forcing one spectra to show significant spectral flattening below 40 keV. For this analysis, the westerly background spectra and corresponding source spectra are not used for energy bins below 40 keV.

The data reported here are for three different pointing directions (Figure 1): 48 hrs centered on the Galactic Center ($l=0^\circ$, $b=0^\circ$), 4 hrs on GRO J1655-40 ($l=-14.6^\circ$, $b=1.8^\circ$), and 23 hrs on the Galactic Plane ($l=-25^\circ$, $b=0^\circ$).

3. Conversion to Photon Spectra

The source and background counts were gain and livetime corrected, and then binned into 42 channels from 20 keV to 17 MeV for each separate FOV. A narrow interval around the neutron-induced instrumental line at 198 keV was excluded due to its variability, and the 511 keV line subtraction was performed in a separate analysis (Boggs 1998). The rest of the lines were either weak enough or varied slowly enough that they required no special treatment.

The corresponding background is subtracted from each source observation and the residual count spectra are corrected for atmospheric attenuation and detector response by a procedure equivalent to directly inverting the coupled atmospheric/detector response matrix. Matrices were modeled for a range of atmospheric column densities using a Monte Carlo simulation of a thin atmosphere above the HIREGS instrument, then normalized to calibration measurements performed before the flight (Boggs 1998). For the exact column density of any source observation, the response matrix is interpolated from the models.

All of the photon spectra for a given pointing direction are then weighted and averaged into a single spectrum for each FOV. These spectra are weighted by the product of livetime and atmospheric transmission, which is an energy-dependent factor that is proportional to the expected signal-to-noise. Spectra are weighted by this factor instead of the measured signal-to-noise so as not to bias the average towards those spectra where statistical fluctuations have resulted in a higher signal.

4. Determination of Compact Sources

The hard X-ray (30-200 keV) photon flux for each of the 12 FOVs is shown in Figure 2. The flux has been corrected for the detector response and the atmospheric transmission, but not for the angular response of the main collimator or the narrow collimators. Therefore, these rates are the sum of the diffuse and compact sources in the Galactic Center region convolved through the angular response of the instrument for each separate FOV.

The wide (21°) FOVs [0,4,8] are large enough that this flux will be a combination of possibly several compact sources plus a strong contribution from the diffuse Galactic continuum. The narrow ($3.7^\circ \times 21^\circ$) FOVs [1-3, 5-7, 9-11] are oriented relative to the Galactic Plane such that a compact source (or multiple sources) within one of these FOVs

will dominate over the diffuse flux, and thus permit identification of the compact sources and their intensities. The problem is to determine the number of compact sources, their locations, and their fluxes — as well as the diffuse component distribution and flux.

The approach taken here is to assume that the possible compact sources observed must be among the previously known hard X-ray sources in the Galactic Center region. Figure 1 shows the 10 known sources used in this analysis. The hard X-ray sources, however, are highly variable — any combination of the sources could be contributing to the observations; therefore, nothing is assumed about the source intensities except that they have to be positive.

These ten compact source locations were convolved through the angular response for each FOV to determine a response array for each source (Figure 3). The contribution of any source to the overall photon rates (Figure 2) is given by the response array for that source multiplied by the source flux. (The response arrays are actually energy dependent, but vary little below 200 keV where the main and narrow collimators are nearly opaque.) Each source has a unique response array, which allows deconvolution of the source contribution to the measured fluxes.

The assumed model for the Galactic diffuse continuum is that the flux comes entirely from the Galactic Plane, the scale height of this distribution is much less than the 21° FOV, and that the longitudinal distribution is flat for the range of observations here ($-35^\circ < l < 10^\circ$). The resulting distribution is a line of constant flux along the Galactic Plane. The assumption of a constant longitudinal distribution is based on previous observations of a Galactic ridge extending $\pm 60^\circ$ in longitude in the hard X-ray and soft gamma-ray bands (e.g., Wheaton 1976, Worrall et al. 1982, Koyama et al. 1989, Gehrels & Tueller 1993, Strong et al. 1996, Purcell et al. 1995, Valinia & Marshall 1998), and will be shown to be consistent with this observation as well.

The narrow Galactic Plane distribution was convolved through the angular response for each FOV to determine a response array for the diffuse component. This response array differs in units from the compact source array since it is expressed as the effective angular extent of the Galactic Plane through each FOV (Figure 3). The contribution of the diffuse flux to the overall photon rates (Figure 2) is given by this response array multiplied by the Galactic Plane flux, which is measured in $[ph/cm^2/s/rad]$.

Given the set of 10 compact source and the Galactic diffuse response arrays, it remains only to find the combination of compact source (CS) and Galactic Plane diffuse (GP) intensities which, when multiplied by the appropriate response arrays, best fit the observed rates in Figure 2. Statistically, with 12 data points and 11 intensities to fit, there is only one remaining degree of freedom to judge the fit. Instead of trusting this fit, especially with the errors on these observations, a more systematic and physical approach is applied.

The hard X-ray sources are highly variable, and often below the level of detection. Given this variability, the approach we have taken to determine the compact sources is to try an increasingly complex systematic combination of source models $GP + nCS$ ($n = 0, 1, \dots, 10$), where we increase the number n of compact source combinations until a good fit is determined.

The first acceptable fits, which are also very good fits, occur for the combination $GP + 3CS$ model. There are actually four combinations of three compact sources which give acceptable fits. All of these combinations have the sources GRO J1719-24 and 1E1740-2942 in common, but four choices of the third source give acceptable fits: GRO J1655-40 [$\chi^2_\nu = 5.40, \nu = 8$], OAO 1657-415 [5.55,8], GX 340+0 [6.29,8], 4U1700-377 [9.95,8].

These four sources are located within 10° of each other, and all lie along a line roughly parallel to the narrow collimator orientation (Figure 1), which explains why they could be confused in this analysis. While these measurements cannot absolutely determine which of

the compact sources is the actual third source, there are two strong reasons to believe that this source is the marginally best-fit source, GRO J1655-40.

The first reason is that GRO J1655-40 was reported as undergoing a small flare during the period of this balloon flight, as determined by BATSE using occultation techniques (Harmon et al. 1995). The second reason is due to the spectral results below. This third compact source has a very hard spectrum, with a power-law ($\alpha = 2.3$) showing no sign of a spectral break below 330 keV. This hard spectrum is characteristic of black hole candidates. Of the four candidate sources, OAO 1657-415, GX 340+0, and 4U1700-377 are all neutron star binaries, while GRO J1655-40 is one of the strongest black hole candidates (Bailyn et al. 1995). The spectrum supports the conclusion that GRO J1655-40 is the third compact source in these observations.

The best-fit combination of the response arrays for this model is shown in Figure 2. The overall fit is excellent [$\chi^2_\nu = 5.40$, $\nu = 8$], with the individual flux rates given in Table 1. The uncertainties on these flux rates are determined by varying the individual source intensities in the model fit independently until $\delta\chi^2 = 1$.

5. Spectral Decomposition

To determine the individual spectra of these sources, one would like to perform the same analysis as above, only using smaller energy bands, extending the analysis from 30 keV to 800 keV (the upper limit of good statistics), and assuming the four sources ($GP + 3CS$) instead of deriving them. This analysis, however, tends to produce large fluctuations, and hence spectral features, that are clearly not real, an excess in one source spectrum having a corresponding drop in another. The measured spectra in the 12 FOVs are fairly smooth (Figure 4), exhibiting no obvious spectral features. Therefore, it is natural to assume that

the source spectra themselves are smooth, that spectral features in the sources are not combining in a way to produce overall smooth measured spectra.

In order to keep the source spectra smooth, we assume spectral models for the four sources, and then determine the best-fit parameters of these models. For the three compact sources we assume power-laws with exponential breaks:

$$f(E) = f(E_o)(E/E_o)^{-\alpha}e^{-(E-E_o)/E_{break}}, (E_{low} < E < E_{high}), \quad (1)$$

where the spectral index α , exponential break E_{break} , and normalization $f(E_o)$ are free parameters of the fit. This is a good general function because it can fit both a pure power-law ($E_{break} > E_{high}$), or a thermal bremsstrahlung ($\alpha \simeq 1.3 - 1.5$).

For the diffuse continuum, we assume a single power-law plus positronium continuum, where the normalization of the two components is allowed to vary independently. There are two issues concerning this fit which should be addressed immediately. The first issue arises because of the assumed single power-law — whereas several observations have shown a spectral break or steepening in the hard X-ray range (Gehrels & Tueller 1993, Purcell et al. 1995) which forcing a single power-law fit will not duplicate. The ultimate test of this fit is the χ^2 . The fitting methods below turns out to be very robust for this data, in the sense that if a "wrong" fit is forced, the χ^2 grows very quickly. We also confront this problem directly, however, by performing the spectral deconvolution twice, in the overall energy range (30-800 keV), and also in just the hard X-ray range (30-200 keV), and confirming the consistency of the fit over the entire soft gamma-ray range.

The second issue concerns our use of a single incident positronium flux for all the FOVs of the instrument. While there has been evidence for a flat Galactic ridge for the power-law component, the same is not true for the positronium continuum. Our deconvolution, therefore, fits the average positronium continuum, not accounting for a gradient. This fit is justified, as will be shown, because our measurements indicate that the gradient is less

than our uncertainty for this component.

Using reasonable initial estimates of the spectral shapes and intensities, we apply a relaxation procedure to determine the best estimates of these spectra consistent with every FOV. An improved estimate of each source (compact or diffuse) is obtained by subtracting all of the other estimated source fluxes convolved through the collimator response from each FOV, then finding the best-fit spectrum to the residuals consistent with the angular efficiency of the source in each FOV. This spectrum is used as the new best estimate for the source, and the procedure is then repeated on the next source. This procedure is iterated until the source fits have stabilized and the χ^2 's are minimized. This technique is stable to initial estimates and order of permutation. It is also sensitive to spectral models — with 397 degrees of freedom, spectral models that are forced (i.e. wrong shapes, parameters) quickly give unacceptable χ^2 's.

The overall goodness of the fits are determined by convolving the best-fit model spectra through the angular response of the instrument for each FOV, and finding the χ^2 fit to the 12 measured spectra simultaneously (Figure 4). Uncertainties were determined by varying the parameters independently until $\delta\chi^2 = 1$. The spectral models fit the observations very well, with an overall $[\chi^2_\nu = 392.1, \nu = 397]$, which gives a 56% probability that the four model spectra agree with the observations.

The best spectral fits to the compact sources are given in Table 2. 1E1740-2942 is the weakest of the sources, and shows a spectral break near or just below the lower energy range (30 keV) of our observations, which makes the spectral index highly uncertain; therefore, it is assumed that the index fits a thermal bremsstrahlung ($\alpha = 1.4$). The spectra for these compact sources are all consistent with black hole candidates, and support the validity of the spectral decomposition process.

The Galactic diffuse spectrum is well fit by a power-law with photon spectral index

$\alpha = (1.80 \pm 0.25)$, $f(70\text{keV}) = (1.95 \pm 0.28) \times 10^{-4} \text{ ph/cm}^2/\text{s/rad/keV}$, and a positronium continuum flux $(1.24 \pm 0.30) \times 10^{-2} \text{ ph/cm}^2/\text{s/rad}$ (Figure 5). The measured 511 keV flux from the Galactic Center is $(1.25 \pm 0.52) \times 10^{-3} \text{ ph/cm}^2/\text{s}$, the analysis of which is presented elsewhere (Boggs 1998). This spectral index is consistent with CGRO/COMPTEL measurements at higher energies (Strong et al. 1996), and RXTE measurements at lower energies (Valinia & Marshall 1998).

6. Self-Consistency Analysis

In order to determine whether there is any evidence for a hard X-ray spectral break or steepening in the diffuse continuum, the above analysis was repeated for just the hard X-ray spectra (30-200 keV). If the Galactic diffuse does steepen in the hard X-ray range, then the power-law index for this fit should be significantly softer than the index for the entire energy range fit. The best-fit Galactic diffuse hard X-ray spectra (30-200 keV) has index $\alpha = (2.03 \pm 0.32)$ with $f(70\text{keV}) = (1.89 \pm 0.28) \times 10^{-4} \text{ ph/cm}^2/\text{s/rad/keV}$. This fit is consistent with the previous results over the entire range (30-800 keV), and therefore these observations show no evidence for spectral steepening in the hard X-ray range.

Furthermore, this measurement strongly rules out the best-fit spectrum determined by OSSE/CGRO observations in conjunction with SIGMA (Purcell et al. 1995). Figure 6 shows the best-fit parameters and uncertainty curves for the (30-800 keV) fit. Shown for comparison are the parameters for the OSSE/CGRO hard X-ray results. As can be seen, this measurement is inconsistent with the OSSE/CGRO results at $\delta\chi^2 > 100$ (only taking into account the uncertainties on this measurement), corresponding to a probability of consistency of $< 10^{-6}$.

As a check on the spectral deconvolution, the model fits are integrated over the range

(30-200 keV) and the fluxes are compared to those determined from the source flux rates determined in Section 4. The results of these integrations are given in Table 1. The model spectra are consistent with the directly deconvolved hard X-ray fluxes for all four sources.

Given the best-fit spectral models, we can subtract the compact source contribution from each FOV and determine whether the assumption of a flat Galactic ridge distribution, both for the power-law and the positronium continuum, is justified. The compact source spectra were convolved through the instrument response and subtracted from the flux in each FOV. Then, the remaining diffuse flux is determined for each FOV separately. The flux rates in each FOV can then be compared, and gradients determined.

Using this technique, the diffuse hard X-ray (30-200 keV) flux shows a gradient of $(1/f)(df/dl) = (-0.30 \pm 0.55) \text{ rad}^{-1}$ which is consistent with a flat distribution. For the positronium flux, the gradient is $(1/f)(df/dl) = (-0.52 \pm 1.19) \text{ rad}^{-1}$ which is also consistent with a flat distribution. Therefore, our assumption of a flat Galactic diffuse distribution is self-consistent with the deconvolved source distribution and fluxes. These measurements place upper limits on the gradient of the components of the diffuse continuum in the central radian of the Galaxy.

7. Discussion

From the measurements presented in this paper, we have concluded that the diffuse emission from the Galactic ridge can be well fit by a single power-law ($\alpha = 1.8$) plus the positronium continuum in the energy range 30-800 keV. The energy flux per logarithmic energy decade, $E^2 f$, for our Galactic diffuse measurements is plotted in Figure 7 along with the COMPTEL/CGRO (Strong et al. 1996) and the RXTE (Valinia & Marshall 1998) observations. From this plot we can see a smooth continuum (plus positronium)

extending from 10 keV up to 30 MeV. However, our normalization is slightly lower than the COMPTEL/CGRO and RXTE results, which is most likely due to our assumption that the latitude distribution of the diffuse emission is very narrow. For a broad latitude distribution, our overall normalization could be low by factors as large as ~ 2 ; however, the spectral shape is unaffected by this overall normalization factor.

Also included is the bremsstrahlung and inverse Compton model of Strong et al. (1996), which we have smoothly extrapolated from 10 keV down to 3 keV, and to which we have added our measured positronium continuum, and the thermal Raymond-Smith plasma component ($kT = 2.9 \text{ keV}$) measured in the X-ray range by RXTE (Valinia & Marshall 1998). This model fits the diffuse emission measurements well from ~ 20 keV to 30 MeV. With the addition of the π^0 emission (Stecker 1988, Bertsch et al. 1994), this model fits the diffuse well up to ~ 1 GeV (Strong et al. 1996). This model predicts that the HIREGS observations are dominated by the inverse Compton (plus positronium) emission, which is consistent with the large scale-height components measured by COMPTEL/CGRO and RXTE.

This model, however, underestimates the diffuse continuum below 20 keV as measured by RXTE. While it is beyond the scope of this paper to determine the exact nature of this discrepancy, we present two possible explanations. One possibility is that thermal emission from a superhot ISM component could be contributing above 10 keV. Such a component ($kT \simeq 7 \text{ keV}$) was invoked to explain the hard component measured in ASCA observations of the Galactic ridge in the energy range 0.7-10 keV (Kaneda et al. 1998). Given the Galactic disk gravitational potential of $\sim 0.5 \text{ keV}$ (Townes 1989), however, it is not clear how such a superhot component could be confined to the Galactic disk (e.g., Kaneda et al. 1998, Valinia & Marshall 1998).

A more probable explanation is that the measured excess reflects the uncertainties in

the cosmic-ray electron spectrum below 100 MeV. The solar modulation of the cosmic-ray electrons allows direct observation down to only a few GeV (Golden et al. 1984, Golden et al. 1994, Taira et al. 1993), and synchrotron radio emission further constrains the electrons down to 300 MeV (Weber 1983). At lower energies, the cosmic-ray electron spectrum is not constrained by observations. Theoretical calculations have been performed to extend the spectrum to lower energies (e.g., Strong et al. 1995, Skibo & Ramaty 1993), which has in turn been used to estimate the diffuse gamma-ray spectrum. Inverse Compton scattering emission below 20 keV would be predominantly produced by electrons below 100 MeV, so we can turn the argument around to say that the measured hard X-ray spectrum is constraining the cosmic-ray electron spectrum below 300 MeV. Therefore, we interpret the most likely cause of the discrepancy below 20 keV as due to theoretical underestimates of the true cosmic-ray electron spectrum at these previously unconstrained energies.

Our measurements are in strong disagreement with the coordinated OSSE/CGRO and SIGMA observations (Purcell et al. 1995), which show a steepening of the diffuse spectrum in the hard X-ray range ($\alpha = 2.7$). The OSSE/CGRO spectrum would require an anomalously large power ($\sim 10^{43} \text{ erg/s}$) to maintain the electron equilibrium against losses (Skibo, Ramaty & Purcell 1996). One possibility is that the OSSE/SIGMA observations could still be contaminated by significant point source contributions.

Integrating the power-law component of the Galactic diffuse and scaling for a rough model of the Galactic distribution (Skibo & Ramaty 1993) gives a total Galactic power output in the 30-800 keV band of $\sim 6 \times 10^{37} \text{ erg/s}$. Given an efficient emission process, i.e. inverse Compton scattering of interstellar radiation off of cosmic-ray electrons accelerated in supernovae, this power is well within the total power injected to the Galaxy via supernovae, $\sim 10^{42} \text{ erg/s}$ (assuming 10^{51} erg every 30 yr).

8. Conclusions

HIREGS observations of the Galactic Center region, by combining wide and narrow FOVs simultaneously, allow separation of the Galactic diffuse continuum and the compact source contributions, from $(-35^\circ < l < 10^\circ)$. The resulting diffuse soft gamma-ray spectrum is found to be hard ($\alpha = 1.8$) down to 30 keV. The Galactic Plane distribution is found to be flat in this longitude range (Galactic ridge) with no sign of an edge, and upper limits are set on the gradients of the diffuse components in this region.

Comparison of the diffuse spectrum with the model of Strong et al. (1996) suggests that we are predominantly measuring the inverse Compton emission, in addition to the positronium continuum. The inverse Compton model is consistent with the large scale height components measured by COMPTEL/CGRO and RXTE in the neighboring energy bands, and with the smooth continuum measured from ~ 20 keV to 30 MeV. By minimizing the need to invoke inefficient nonthermal bremsstrahlung emission in the hard X-ray range, these measurements require only a small fraction of the power provided by Galactic supernovae. Discrepancies between the model and the measurements below 20 keV are most likely due to theoretical underestimates of the cosmic-ray electron spectrum below 100 MeV; therefore, the diffuse hard X-ray/soft gamma-ray spectrum is providing the first direct constraints on the cosmic-ray electron spectrum below 300 MeV.

Given these conclusions, further measurements of the diffuse hard X-ray/soft gamma-ray emission, both its spatial and spectral distributions, are crucial to separate the various components of the emission and better constrain the cosmic-ray electron spectrum below 300 MeV. Furthermore, these conclusions suggest that nonthermal components extending from the hard X-ray into the soft X-ray bands should be analyzed in terms of constraining the cosmic-ray electron spectrum to even lower energies, dominated by inverse Compton scattering emission.

We are grateful to R. Ramaty for useful discussions, and A. Valinia for providing the RXTE data. This research was supported in part by NASA grant NAGW-3816.

	Measured	Spectral Fit
GP diffuse ^a	3.28 ± 0.40	2.63 ± 0.36
GRO J1655-40 ^b	3.19 ± 0.31	3.58 ± 0.32
GRO J1719-224 ^b	7.72 ± 0.34	8.23 ± 0.43
1E1740-2942 ^b	1.98 ± 0.21	1.72 ± 0.21

Table 1: Source Flux [30-200 keV].

^a $[10^{-2}ph/cm^2/s/rad]$

^b $[10^{-2}ph/cm^2/s]$

	$f(70 \text{ keV})^a$	α	$E_{break} \text{ [keV]}$
GRO J1655-40	2.72 ± 0.22	32.19 ± 0.17	> 330
GRO J1719-224	5.86 ± 0.22	1.46 ± 0.08	44.3 ± 2.9
1E1740-2942	0.99 ± 0.10	1.4^b	28.9 ± 3.4

Table 2: Compact Source Spectral Fits.

^a $[10^{-4}ph/cm^2/s/keV]$

^bdefined (see text)

REFERENCES

- Bailyn, C. D. et al., 1995, *Nature*, 378, 157
- Bertsch, D., et al. 1994, *ApJ*, 416, 587
- Boggs, S. E. 1998, Ph.D. Dissertation, University of California, Berkeley
- Boggs, S. E., et al., 1997, *The Transparent Universe*, 2nd INTEGRAL Workshop, ESA SP-382, 153
- Boggs, S. E., et al. 1998, *Adv. Space Res.*, 21, 1015
- Gehrels, N., & Tueller, J. 1993, *ApJ*, 407, 597
- Golden, R. L. et al., 1984, *ApJ*, 287, 622
- Golden, R. L., et al. 1994, *ApJ*, 436, 769
- Harmon, B. A., et al. 1995, *IAU Circ.*, 6147
- Harris, M. J., et al. 1990, *ApJ*, 362, 135
- Kaneda, H., et al. 1997, *ApJ*, 491, 638
- Koyama, K., et al. 1989, *Nature*, 339, 603
- Pelling, R. M., et al. 1992, *SPIE*, 1743, 408
- Purcell, W. R., et al. 1995, *Proc. 24th ICRC*, 2, 211
- Skibo, J. G. 1997, *The Transparent Universe*, 2nd INTEGRAL Workshop, ESA SP-382, 555
- Skibo, J. G., & Ramaty, R. 1993, *A&AS*, 97, 145
- Skibo, J. G., Ramaty, R., & Purcell, W. R. 1996, *A&AS*, 120, 403

- Stecker, F. W. 1988, Cosmic Gamma Rays, Neutrinos and Related Astrophysics, eds. M. M. Shapiro & J. P. Wefel (Dordrecht: Reidel), 85
- Strong, A. W., et al. 1995, Proc. 24th ICRC, 2, 234
- Strong, A. W., et al. 1996, A&AS, 120, 381
- Taira, T., et al. 1993, Proc. 23rd ICRC, 1, 333
- Townes, C. H. 1989, IAU Symp., 136, The Center of the Galaxy, ed. M. Morris (Dordrecht: Kluwer), 1
- Valinia, A., & Marshall, F. E. 1998, ApJ, 505, 134
- Webber, W. R. 1983, in Composition and Origin of Cosmic Rays, Shapiro, M. M. (ed.), D. Reidel, 83
- Wheaton, W. A. 1976, Ph.D. Dissertation, University of California, San Diego
- Worrall, D. M., et al. 1982, ApJ, 255, 111
- Yamasaki, N. Y., et al. 1996, A&AS, 120, 393

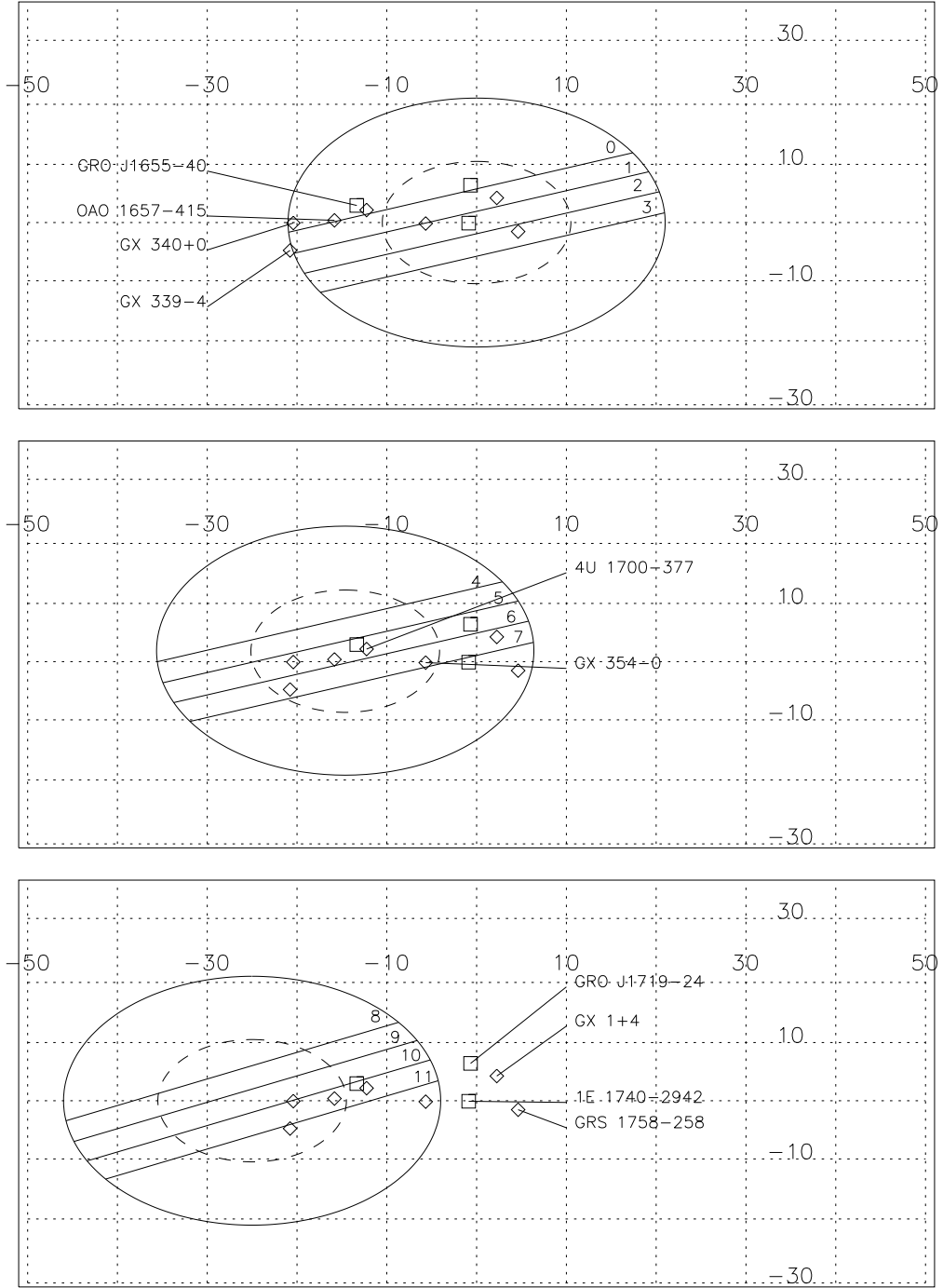


Fig. 1.— The HIREGS observations in the Galactic Center and Plane ($-35^\circ < l < 10^\circ$). The 12 FOVs are numbered 0-11 for reference. Also shown are the 10 trial compact sources used to deconvolve the data. The three compact sources (all black hole candidates) that this analysis shows were active are marked with squares.

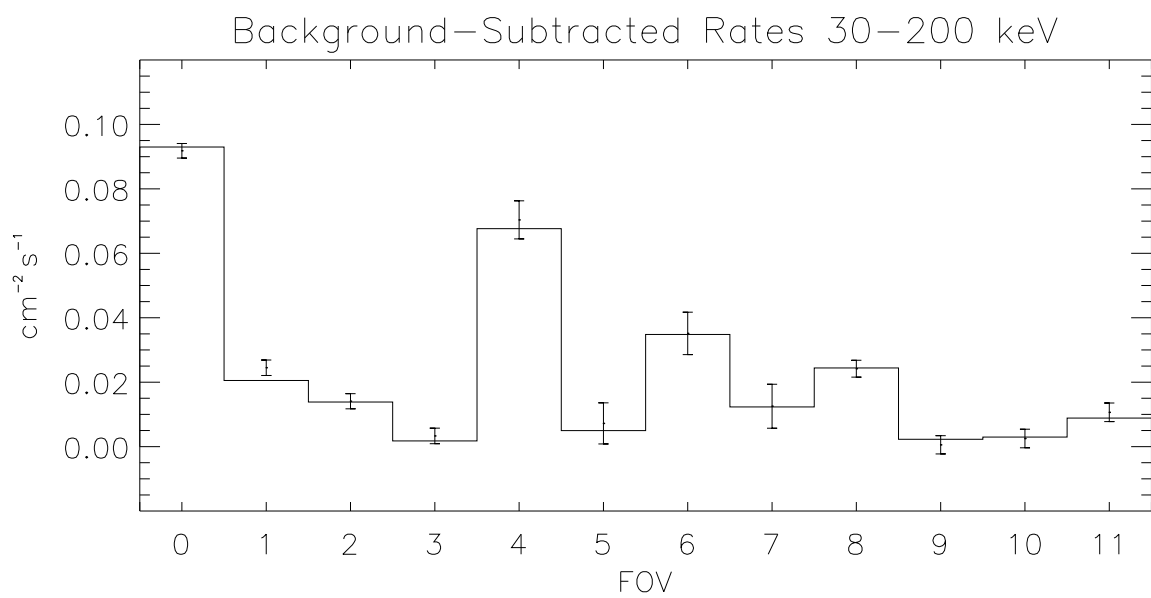


Fig. 2.— The hard X-ray flux for the 12 FOVs shown in Figure 1. Also shown (solid line) is the best-fit fluxes for the Galactic diffuse, GRO J1719-24, 1E1740-2942, and GRO J1655-40 convolved through the angular response for each FOV [$\chi^2_\nu = 5.40$, $\nu = 8$].

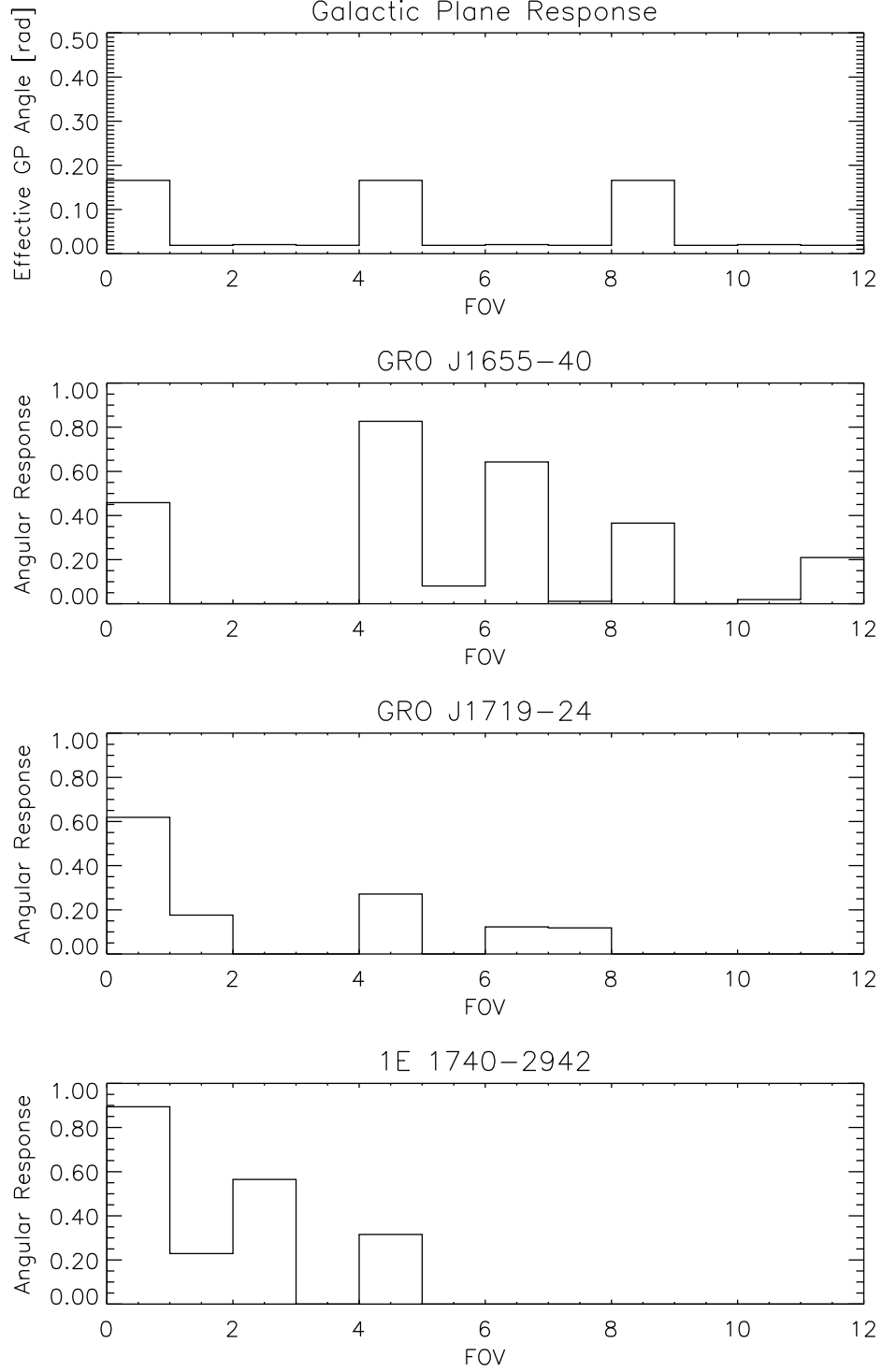


Fig. 3.— The angular response for each FOV for the 3 best-fit compact sources in Figure 1, and the Galactic Plane assuming a narrow ridge distribution. Each source has a unique response array, which allows deconvolution of the compact sources and the Galactic diffuse flux.

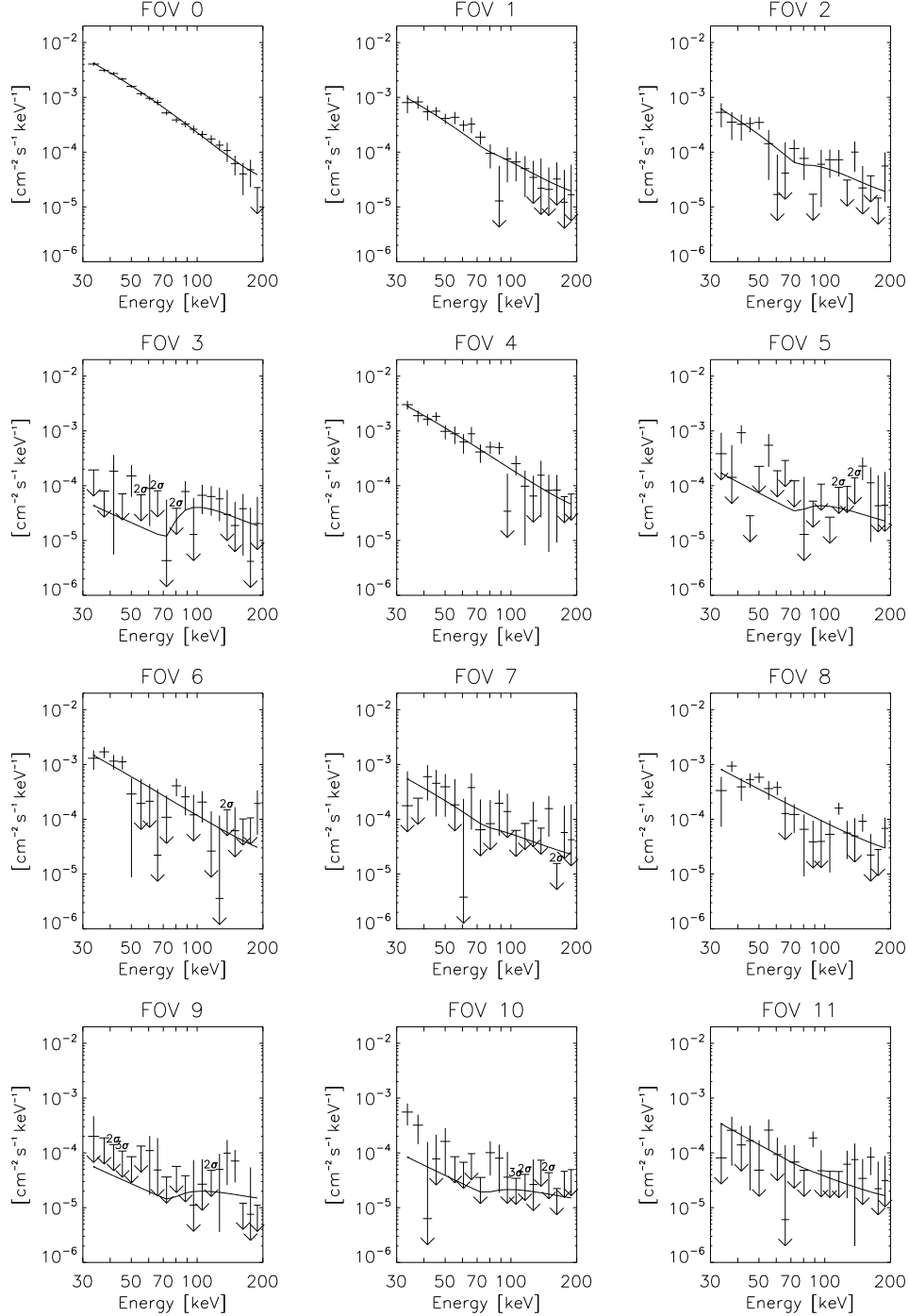


Fig. 4.— The hard X-ray photon spectra for the 12 FOVs shown in Figure 1. Also shown (solid lines) are the best-fit spectral models for the Galactic diffuse, GRO J1719-24, 1E1740.7-2942, and GRO J1655-40 convolved through the angular response for each FOV [$\chi^2_\nu = 392.1$, $\nu = 397$]. All limits are 1σ unless noted.

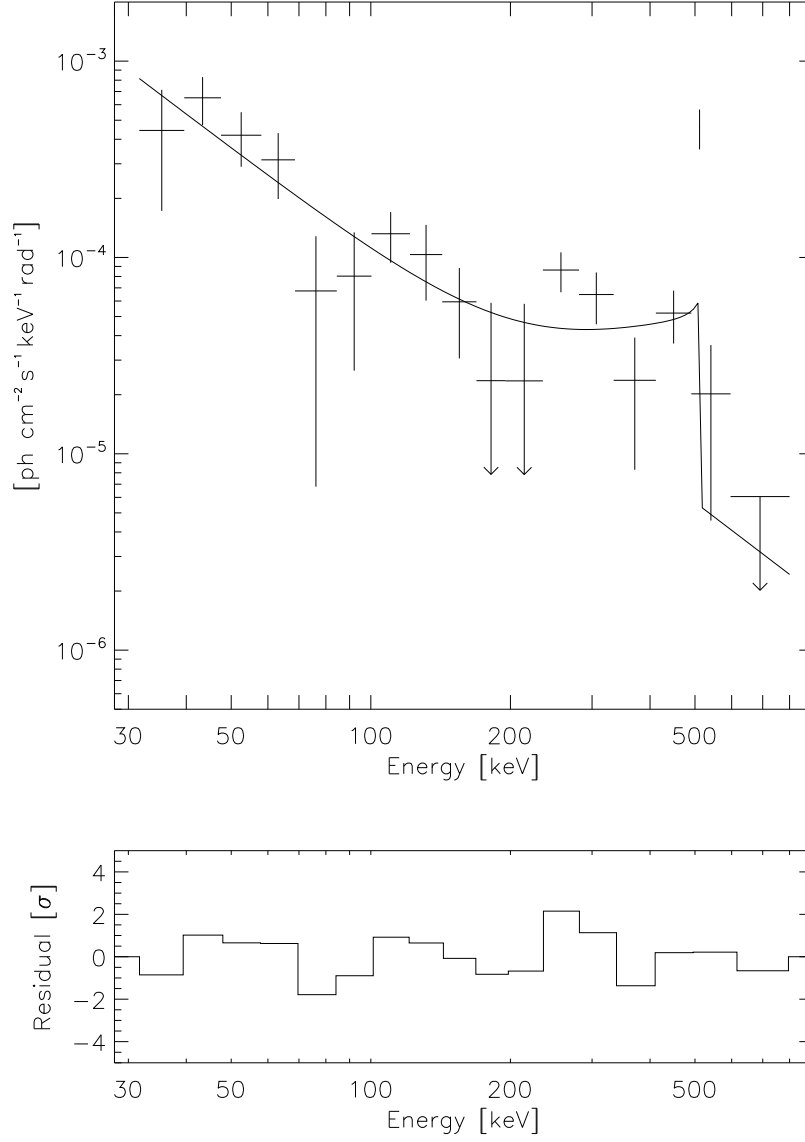


Fig. 5.— The compact-source corrected Galactic diffuse continuum. The best-fit spectrum (solid line) is shown. The 511 keV measurement is discussed in Boggs (1998).

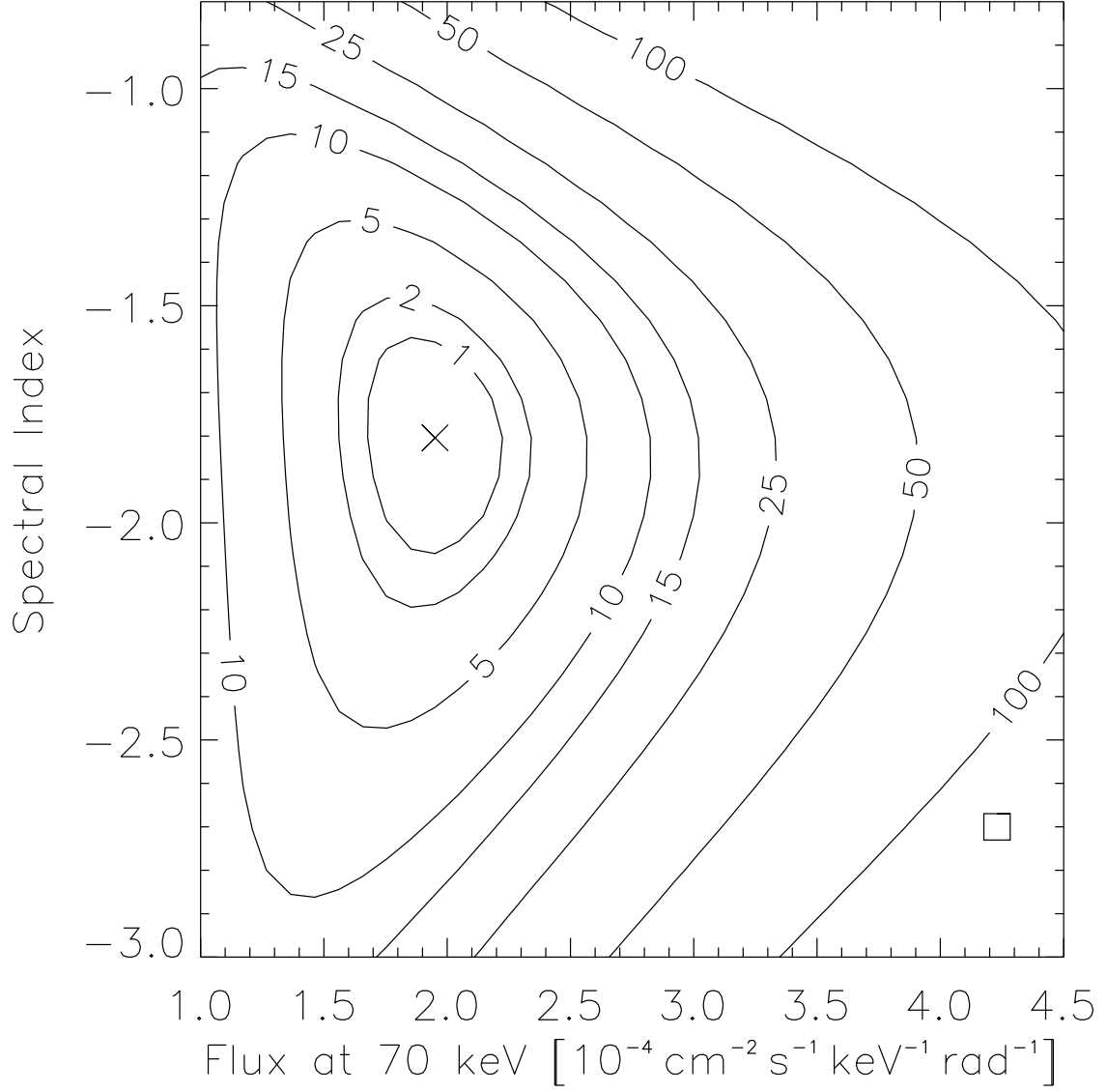


Fig. 6.— The spectral parameter $\delta\chi^2$ curves for the (30-800 keV) diffuse continuum. Shown for comparison (square) is the best-fit OSSE/CGRO hard X-ray spectral parameters (Purcell et al. 1995), which are inconsistent with these measurements at the $\delta\chi^2 > 100$ level.

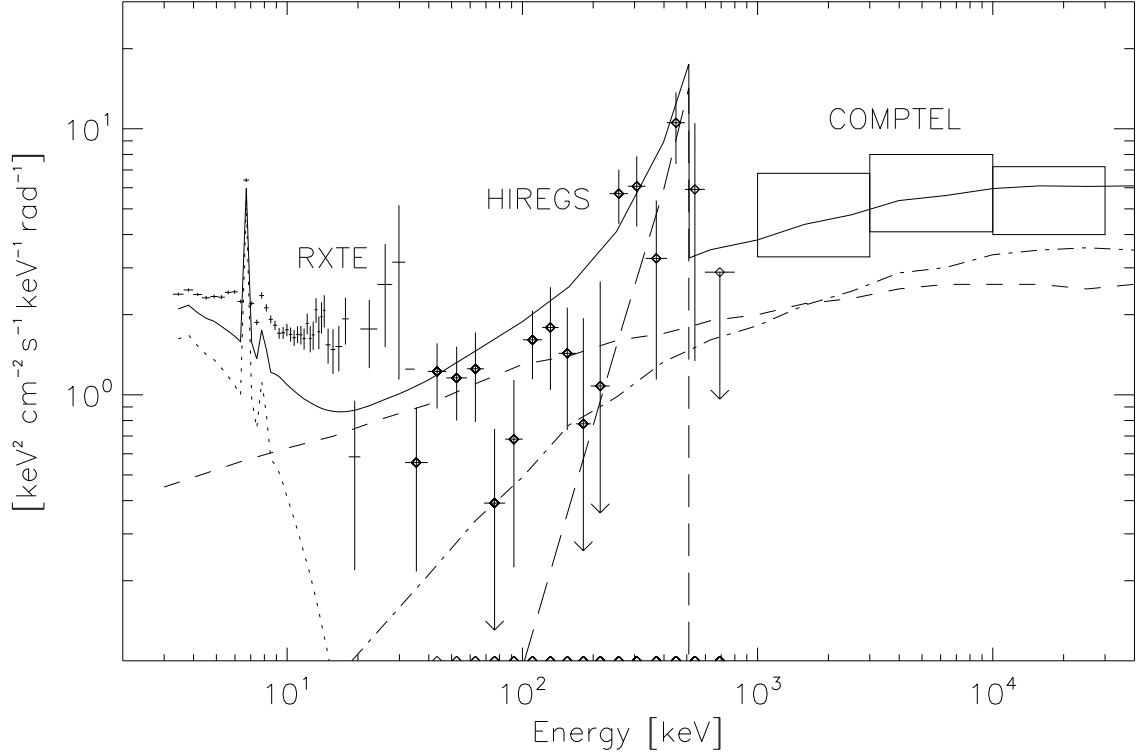


Fig. 7.— The hard X-ray/soft gamma-ray Galactic diffuse emission (RXTE - Valinia & Marshall 1998, COMPTEL/CGRO - Strong et al. 1996). Also shown is the bremsstrahlung (dot-dashed line) and inverse Compton scattering (short dashed line) model of Strong et al. (1996), with the HIREGS measured positronium continuum (long dashed line) and the thermal Raymond-Smith plasma component (dotted line) measured in the X-ray range by RXTE (Valinia & Marshall 1998) added. The total of the model components is also presented (solid line).